



Evaluating the dependency of polymer/particle interphase thickness to the nanoparticles content, aggregation/agglomeration factor and type of the exerted driving force

Esmail Sharifzadeh¹

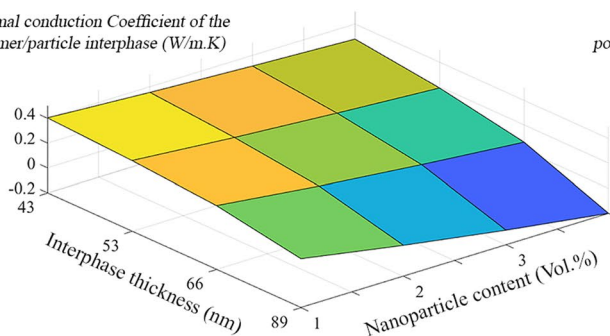
Received: 27 February 2021 / Accepted: 29 May 2021 / Published online: 8 July 2021
© Iran Polymer and Petrochemical Institute 2021

Abstract

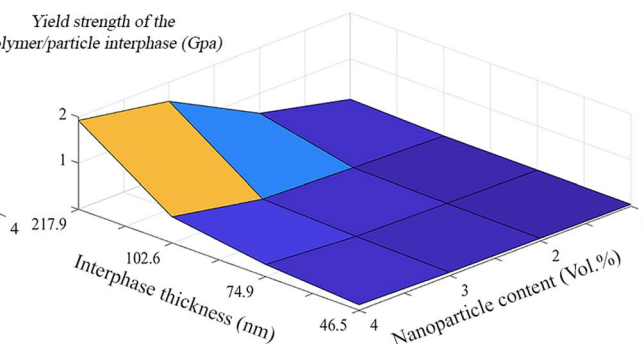
The physical/mechanical characteristics of the polymer/particle interphase region have been always considered to be dependent on the surface chemical structure of the nanoparticles and their interactions with the polymer chains. In addition, it is repeatedly reported that the interphase-related parameters (e. g., thickness, tensile modulus and strength, yield strength, thermal conductivity) can be considered constant under any process conditions. Accordingly, in this study, a comprehensive investigation was performed to define the effects of nanoparticles content, aggregation/agglomeration factor and type of the exerted driving force on the characteristics of the polymer/particle interphase region. To this end, different experimental/analytical approaches were adapted by which it was possible to precisely characterize the internal structure of PS/silica and PMMA/silica nanocomposite samples based on their thermal and mechanical properties. The mechanical characteristics were evaluated using a developed form of Zare's model and in the case of thermal characteristics, two new analytical models were proposed based on equivalent box model (EBM). According to the results, it was revealed that the increment of the nanoparticle content increased the thermal conductivity of the interphase while decreased its thickness and yield strength. Moreover, it was found that the aggregation/agglomeration of nanoparticles had negative effects on the interphase thermal properties which were negligible at low contents.

Graphic abstract

Thermal conduction Coefficient of the polymer/particle interphase (W/m.K)



Yield strength of the polymer/particle interphase (Gpa)



Keywords Polymer/particle interphase · Aggregation/agglomeration · Polymer nanocomposites · Thermal/mechanical characteristics · Thermal conduction

✉ Esmail Sharifzadeh
E.sharifzadeh@razi.ac.ir

¹ Polymer Research Center, Faculty of Petroleum and Chemical Engineering, Razi University, Kermanshah, Iran

Introduction

Investigation of the mechanical properties and thermal conductivity of polymer composites/nanocomposites has been always considered a very important field due to the wide

application of this family of materials in different industries [1–3]. Polymer composites are expected to have the best consistency with the process conditions which is crucial to utilize the most precise methods in their designing stage [4, 5]. In general, there are two main procedures: (I) direct application under simulated environmental conditions and (II) modeling approaches to evaluate the performance of the designed products [6–8]. The direct application of the composites/nanocomposites, to evaluate their probable consistency with the conditions, is not a cost/time effective method, while the modeling approach can provide valuable and practical results very fast and with almost no cost. There are many theoretical, semi-empirical and empirical models which have been developed so far. They consider a variety of assumptions to aim to elevate the level of understanding of how the thermal/mechanical characteristics of polymer composites/nanocomposites are dependent on different factors [9–11].

In the case of polymer nanocomposites, regardless of the shape and content of the nanoparticles, presence of the polymer/particle interphase regions somewhat complicates the modeling process [12–14]. It is well-understood that the characteristics of the interphase region drastically affect the network properties of the system due to the relatively large size of the region compared to the size of the fillers [13, 15]. Though it is impossible to define the characteristics of the polymer/particle interphase regions via direct measurement methods and, therefore, using the indirect methods, modeling approaches, is the only choice to obtain information about this important part of the nanocomposites [16, 17]. The polymer/particle interphase regions are formed based on the adsorption of the polymer molecules onto the surface of the nanoparticles [12, 13, 18]. This can be ascribed to the mutual interaction between the chemical sites on the surface of the nanoparticles with specific groups of the polymer chains [12, 17]. Jain et al. have reported that the nanoparticles selectively adsorb the highest molar mass polymer chains, during the production process, while the surrounding matrix contains low molar mass polymer chains [18]. In addition, according to De Genne's scaling theory of polymer adsorption, the density of the interphase region decreases with the distance from the surface of the nanoparticles until it equals the density of the polymer matrix [19–21].

Accordingly, the inevitable formation and thermal/mechanical characteristics of the polymer/particle interphase regions significantly affect the heat transfer and stress transfer in polymer nanocomposites [22, 23]. Moreover, the aggregation/agglomeration of the nanoparticles can be introduced as another important parameter that drastically affects their performance in the system [24–26].

Different variation patterns, as a function of distance from the surface of the nanoparticle, can be considered for physical/mechanical properties inside the interphase regions (e.

g., linear and exponential) [14, 27, 28]. All of the mentioned patterns have one thing in common according to which the variation starts from a maximum value, on the surface of the nanoparticle, and ends to a minimum value, equal to the value of the corresponding property in the polymer matrix [14, 27]. As it is clear, the thickness of the interphase is a very important parameter by which it is possible to determine the average value of the physical/mechanical properties for the interphase region. For instance, Ji et al. have proposed the following equation to calculate the tensile modulus of the interphase region [14]:

$$dE_i = \frac{E_{i0} - E_m}{\tau} dl, \quad (1)$$

where E_{i0} denotes the maximum tensile modulus on the surface of the nanoparticles, E_m is the tensile modulus at end of the interphase region ($E(\tau)$), τ represents the thickness of the interphase and l is the distance from the surface of the nanoparticles.

The effects of the polymer/particle interphase region on the physical/mechanical properties of the polymer nanocomposites have been widely investigated. Zare et al. have investigated the effects of the interphase and filler size on the percolation threshold of carbon nanotubes in nanocomposites [21]. Maghami et al. have proposed a new method to characterize the polymer/particles interphase using the gas permeability method [17]. In another study by Wan et al., the combination of microstructure characterization and micro-mechanical modeling methods has been used to evaluate the effects of the polymer/particle interphase region on the mechanical properties of the polymer/graphene oxide nanocomposites [17]. Furthermore, we have previously proposed many methods to characterize the physical/mechanical properties of the polymer/particle interphase regions in different nanocomposite systems [26, 29, 30].

In almost all related studies, the interphase region is introduced as a specific solid part of the nanocomposite, with specific characteristics, whose formation is not dependent on other system parameters [13, 14, 31]. Accordingly, a comparative study was performed to evaluate and compare the obtained values for the polymer/particle interphase thickness based on the thermal and mechanical characteristics of the interphase. The thermal characterization of the interphase was performed using the thermal test results of different prepared nanocomposites samples and a new thermal conduction model considering the effect of the nanoparticle content and aggregation/agglomeration factor. The model was designed based on the combination of series and parallel forms of equivalent box model (EBM) with the corresponding geometrical structure of the nanocomposite system. The mechanical characteristics of the polymer/particle interphase region were determined using a developed form of Zare's model, on the tensile strength of the polymer nanocomposites.

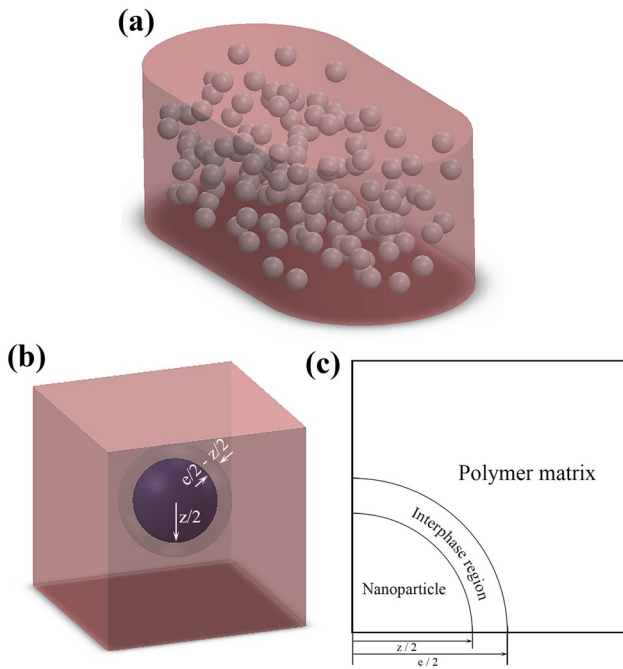


Fig. 1 **a** Structure of polymer nanocomposites containing spherical nanoparticles, **b** corresponding geometrical structure of the system and **c** 2D view of 1/8 of the model structure with distinguished parts

Moreover, tensile, rheology and thermal conduction tests were performed to provide sufficient experimental data for a comprehensive comparison. The tested PS and PMMA nanocomposites, containing 1, 2, 3 and 4 vol% of silica nanoparticles were prepared via melt mixing. Before the mixing process, the nanoparticles were subjected to the chemical surface modification process using (3-aminopropyl)triethoxysilane (APTES) and hexadecyltrimethoxysilane (HDTMS) to enhance their compatibility with PS and PMMA phases, respectively. Thermal conduction and tensile tests were conducted to provide the required experimental results.

Modeling background

Figure 1a demonstrates a schematic of polymer nanocomposite containing spherical nanoparticles that are perfectly dispersed in the matrix. Based on the fundamentals of Ji’s model [14], it is possible to represent the entire nanocomposite structure as a cube, with unit side length, containing a core and shell at its center (Fig. 1b). This geometrical structure is also used by Boutaleb et al. to evaluate the mechanical properties of the polymer nanocomposites containing spherical nanoparticles [32]. It should be noted that the diameter of the sphere (z) and the thickness of the shell ($e/2 - z/2$) are the representatives of the diameter of the nanoparticles and thickness of the actual polymer/particle interphase region, respectively. Accordingly, parameters z and e can be defined using Eqs. (2) and (3), respectively:

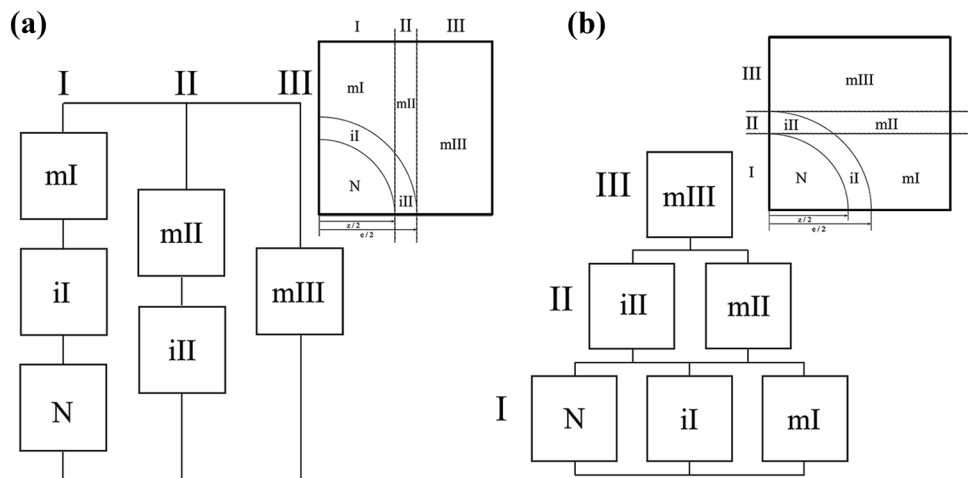
$$z = \sqrt[3]{\frac{3\varphi_d}{\pi 4}} \tag{2}$$

$$e = \sqrt[3]{\frac{3\varphi_d}{4\pi r^3} ((r + \tau)^3 - r^3) + z^3}, \tag{3}$$

where τ is the thickness of the polymer/particle interphase region, φ_d denotes the actual volume fraction of the applied nanoparticles in the nanocomposite samples and r is the radius of the spherical nanoparticles.

As it is illustrated in Fig. 1c, the corresponding geometrical structure of the nanocomposite system (Fig. 1b) can be represented as 1/8 of the main structure which helps to simplify the modeling process. To be more precise, the model structure can be divided into 8 similar and symmetrical parts in which the volume fraction of the constituents is similar to that of the main structure. To evaluate the interaction between the model constituents, it is possible to use two different arrangements of the EBM, as illustrated in Fig. 2.

Fig. 2 Structures of **a** EBMp and **b** EBMs and their relation with their geometrical model structure



In general, EBM constructs a combination of series and parallel boxes, representing model structural constituents, through which it is possible to study the response mechanism of the system against the exerted driving force (e. g., stress, heat, etc.) [14, 26]. Each box in the EBM has a specific volume fraction which in this study should be calculated using the main model structure (Fig. 1b, c) as follows:

$$\varphi_N = 4/3\pi z^3 \quad (4)$$

$$\varphi_{III} = 4/3\pi e^3 - 2 \left\{ \pi \left(e - \sqrt{e^2 - z^2} \right)^2 / 3 \times \left(3 \left(e - \sqrt{e^2 - z^2} \right) - e \right) \right\} - 2\pi^2 \sqrt{e^2 - z^2} \quad (5)$$

$$\varphi_{III} = 4/3\pi(e^3 - z^3) - \varphi_{III} \quad (6)$$

$$\varphi_{mIII} = 1 - \pi e^2 \quad (7)$$

$$\varphi_{mII} = \pi(e^2 - z^2) - \varphi_{III} \quad (8)$$

$$\varphi_{mI} = \pi z^2 - \varphi_N - \varphi_{II} \quad (9)$$

$$\varphi_I = \pi z^2 \quad (10)$$

$$\varphi_{II} = \pi(e^2 - z^2) \quad (11)$$

$$\varphi_{III} = \varphi_{mIII} \quad (12)$$

The thermal resistance along the flux direction is additive [33], and therefore, the effective thermal conduction coefficient of the series component (K_{es}) of the EBMs is

$$R_{Ts} = \sum R_j \rightarrow \frac{1}{K_{es}} = \sum \frac{\varphi_j}{K_j} \quad (13)$$

where φ_j , K_j and R_j are the volume fraction, conduction coefficient and resistance of the component j_{th} . R_{Ts} denotes the overall resistance in the series state.

On the other hand, considering the additive thermal conductance ($C_{Tp} = 1/R_{TC}$) for parallel components it is possible to calculate the effective thermal conduction coefficient of the parallel components (K_{ep}) of the EBMs as follows [33]:

$$C_{Tp} = \sum C_j \rightarrow K_{ep} = \sum \varphi_j K_j \quad (14)$$

In the case of the parallel state of parts I, II and III of the EBM (Fig. 2a), the thermal conduction coefficient of the nanocomposite (K_T) can be calculated using the following equation:

$$K_T = \varphi_I K_I + \varphi_{II} K_{II} + \varphi_{III} K_{III}, \quad (15)$$

where K_I and K_{II} can be calculated using Eqs. (16) and (17), respectively:

$$\frac{1}{K_I} = \frac{\varphi_{mI}}{K_m} + \frac{\varphi_{II}}{K_i} + \frac{\varphi_N}{K_N} (1 - \mu) \quad (16)$$

$$\frac{1}{K_{II}} = \frac{\varphi_{mII}}{K_m} + \frac{\varphi_{III}}{K_i}, \quad (17)$$

where K_N , K_m and K_i denote the conduction coefficient of the nanoparticle, polymer matrix, and polymer/particle interphase region, respectively, μ represents the aggregation/agglomeration factor and $K_{III} = K_m$ (Fig. 2a).

In the case of the series state of parts I, II and III (Fig. 2b) the thermal conduction coefficient of the nanocomposite is

$$K'_T = \left(\frac{\varphi_I}{K'_I} + \frac{\varphi_{II}}{K'_{II}} + \frac{\varphi_{III}}{K'_{III}} \right)^{-1}, \quad (18)$$

where K_I and K_{II} can be calculated using Eqs. (19) and (20), respectively:

$$K'_I = \varphi_{mI} K_m + \varphi_{II} K_i + \varphi_N K_N (1 - \mu) \quad (19)$$

$$K'_{II} = \varphi_{mII} K_m + \varphi_{III} K_i. \quad (20)$$

Hereinafter, the EBM model with parallel and series I, II and III parts will be referred to as EBMp and EBMs, respectively.

Experimental

Materials

Aerosil fumed silica was kindly provided by Degussa (OX-50, $D = 40$ nm, France). (3-Aminopropyl)triethoxysilane (APTES), hexadecyltrimethoxysilane (HDTMS) and ethanol (>99%) were purchased from Merck Co. (Germany) and used without further treatments. Polystyrene (PS) [Grade 1160 GPPS, $\rho = 1.04$ (g/mL)] and poly(methyl methacrylate) [Grade IH830, $\rho = 1.18$ (g/mL)] were purchased from Tabriz Petrochemical (Iran) and LG Co. (South Korea), respectively.

Sample preparation

Surface modification of the nanoparticles to enhance the compatibility with PS and PMMA.

The nanoparticles were added to ethanol and sonicated for 30 min at room temperature, to obtain a well-dispersed suspension, and then APTES was added and the mixture stirred for 24 h. The surface-modified nanoparticles were then collected by centrifugation and washed with water several times to remove extra APTES molecules. Finally, the nanoparticles were dried at 50 °C under vacuum for 24 h. The same method was repeated with HDTMS. The silica nanoparticles modified with APTES and HDTMS were addressed as OXA and OXH, respectively.

Nanocomposite sample preparation

Melt mixing process was performed in an internal mixer (Brabender Plasticorder W50EHT, Germany) (60 rpm, 8 min, 200 °C) to prepare PMMA nanocomposite samples containing 1–4 vol% of OXH nanoparticles. The samples were then transferred to a vacuum oven at 60 °C and after 72 h molded according to ISO-527 using a hot-press device (200 °C, 40 bar). A different mold (thickness: 2 mm, diameter: 20 mm) was also used to prepare suitable samples for thermal conduction and rheology tests. The same method was used to prepare PS nanocomposite samples containing 1–4 vol% of OXA nanoparticles.

Characterization

Rheology test

The frequency sweep rheology tests were conducted using an Anton Paar MCR 301 device (Austria) at 200 °C. The complex and zero shear rate viscosities of the PS-OXA samples were used to interpret the results of the heat conduction tests.

Tensile tests

The tensile tests were performed using a Zwick/Roell tensile testing machine (Z 010, Germany) at room temperature according to ISO-527. At least 3 samples of each composition were tested and the averaged results were used to determine the characteristics of the interphase region based on the developed form of Zare's model.

Heat conduction tests

The thermal conduction coefficient of the tablet-shape nanocomposite samples was measured by placing them between

the heated and cooled metal sections of a heat conduction unit (H940, P.A. Hilton, UK). The heat flux was set at 2 W/m² and then the temperatures at the sides of each sample were read. Finally, Fourier's law [Eq. (21)] was used to calculate the conduction coefficient of the samples [34]:

$$q_x = -k \frac{\Delta T}{\Delta x}, \quad (21)$$

where q_x denotes the heat flux (W m⁻²), ΔT and Δx represent the temperature difference and thickness of the samples, respectively. At least 3 samples of each composition were tested and averaged results \pm STD were reported.

Results and discussion

Table 1 represents the model results regarding the interpreted thermal characteristics of the polymer/particle interphase region based on EBMp (Fig. 2a). As it is clear, the conduction coefficient of the interphase region (K_i) was lower than that of the polymer matrix, in all samples, and decreased with nanoparticles content. This can be ascribed to the higher compactness of the polymer molecules in the region, compared to the surrounding polymer bulk, which decreased the heat transfer [20, 22, 35]. It can be also seen that the thickness of the interphase (τ) and K_i decreased with the nanoparticles content, in both PS-OXA and PMMA-OXH groups, which can be attributed to the selective adsorption of the high molar mass polymer molecules onto the surface of the nanoparticles [18, 35]. The reported values of the aggregation/agglomeration factor (μ) were interpreted from the experimental results via optimizing Eqs. (15) and (18) [15].

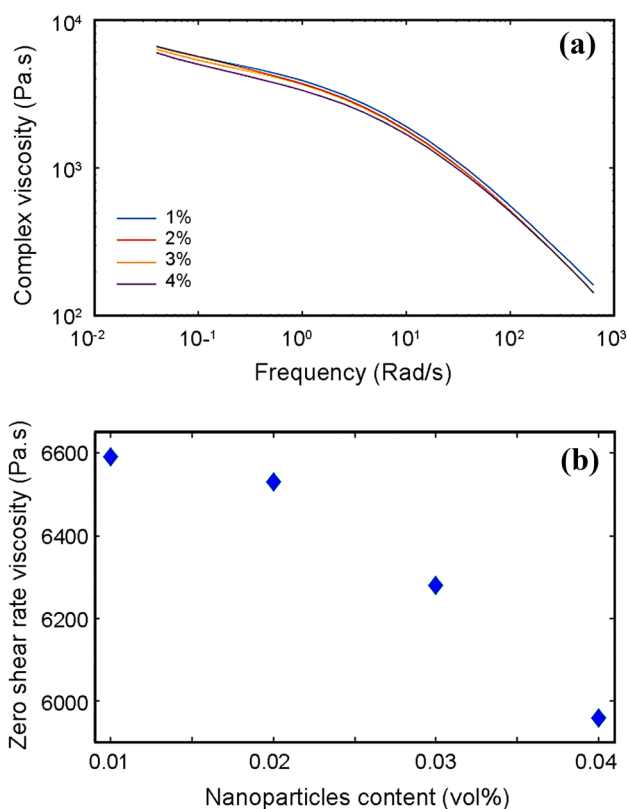
In general, it is reported that the adsorbed high molar mass polymer chains form a shell around the nanoparticles, while the low molar mass chains stay in the surrounding molten matrix [18]. As a result, the increment of the nanoparticle content should decrease the viscosity of the molten nanocomposite. This concept was evaluated via the rheology test using the prepared PS-OXA nanocomposite samples.

As it is demonstrated in Fig. 3a, the complex viscosity ($\eta^*(\omega)$) of the tested samples was decreased with the content of the nanoparticles, whose surfaces were completely compatible with the surrounding polymer phase, at any frequency. Besides, Fig. 3b clearly shows the decrement of the zero-shear rate viscosity with the content of the nanoparticles. These findings are completely similar to those reported in literature [22] and accordingly, it can be concluded that τ is directly dependent on the number and length of the attached polymer chains [18].

Figure 4 represents the schematic of the selective adsorption of the relatively high molar mass polymer chains and its dependency on the nanoparticle content. As it is clear, at

Table 1 Thermal characteristics of the PS-OXA and PMMA-OXH nanocomposite samples based on EBMp

	φ_d (vol%)	(τ) (nm)	(K_i) ($\text{W m}^{-1} \text{k}^{-1}$)	(μ) (%)	Experimental conduction coefficient ($K_{\text{exp.}}$) ($\text{W m}^{-1} \text{k}^{-1}$)	Theoretical conduction coefficient ($K_{\text{the.}}$) ($\text{W m}^{-1} \text{k}^{-1}$)	Error (%)
PS-OXA	0	–	–	–	0.163 ± 0.015	–	–
	1	89	0.143	1	0.196 ± 0.012	0.193	1.5
	2	66	0.148	1.7	0.224 ± 0.016	0.216	3.5
	3	53	0.15	2.6	0.251 ± 0.02	0.241	3.9
	4	43	0.152	3.2	0.283 ± 0.019	0.277	2.1
Average		62.7	0.148	2.05			
PMMA-OXH	0	–	–	–	0.290 ± 0.011	–	–
	1	74	0.23	1	0.425 ± 0.016	0.413	2.8
	2	49	0.241	1.6	0.514 ± 0.014	0.504	1.9
	3	36	0.262	2.8	0.607 ± 0.008	0.598	1.4
	4	26	0.279	3.7	0.698 ± 0.014	0.683	2.1
Average		46.2	0.253	2.275			

**Fig. 3** Rheology test results of PS-OXA nanocomposite samples: **a** variation of the complex viscosity with frequency and **b** variation of zero-shear rate viscosity with the nanoparticle content

first the two big polymer chains were selectively adsorbed (Fig. 4a), while the chains with lower molar mass were not allowed inside the interphase region. However, after the duplication of the available nanoparticles surfaces (Fig. 4b), the increment of the nanoparticles content, there was enough space for other polymer chains, with relatively high molar

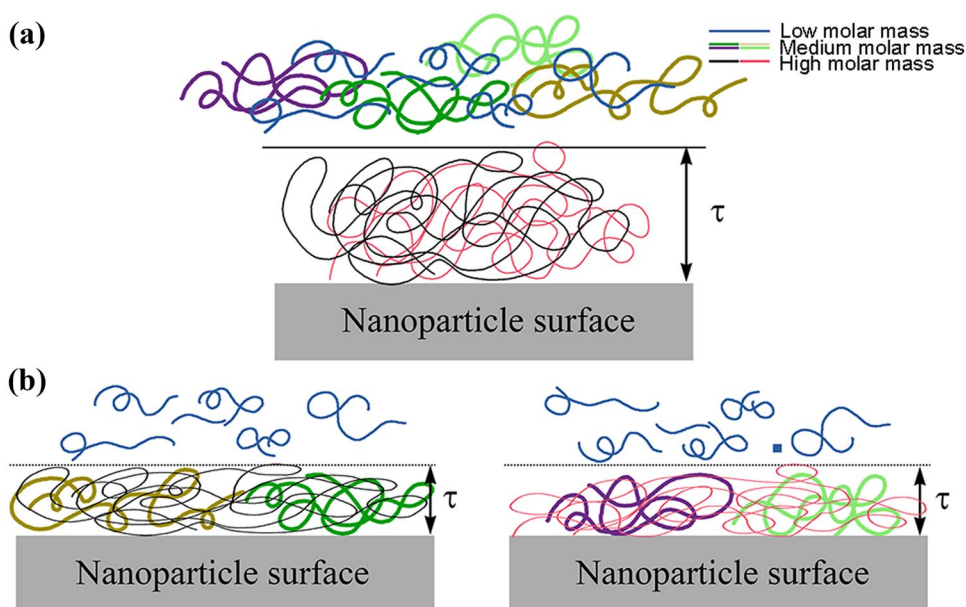
mass compared to other unattached molecules, to enter the interphase region. This increased the length range of the attached chains onto the surface of the nanoparticles and consequently, according to the results of Table 1, decreased the interphase thickness.

The same trends can be also seen for τ and K_i in Table 2, where the interpreted thermal characteristics of the interphase region are represented based on EBMs. Though, it is noteworthy to mention that the average value of K_i was almost the same for PS-OXA or PMMA-OXH samples based on the results of EBMp and EBMs. We have previously proved that the aggregation/agglomeration of the nanoparticles was an inevitable phenomenon, even at very low nanoparticles content (< 1%) [30]. Similar results were also obtained in the present study (Tables 1 and 2). In addition, very low error values of the proposed conduction model, based on both EBM approaches, indicated its acceptable accuracy.

The effects of the variation of parameters τ , K_i and μ on the conduction coefficient of PS-OXA nanocomposite samples [Eqs. (15) and (18)] are represented in Fig. 5. According to both EBM approaches, the increment of K_i at any nanoparticles content increased the conduction coefficient of the nanocomposite (K or K') (Fig. 5b, e). The impact of the aggregation/agglomeration factor (μ) on EBMp was negligible (Fig. 5c), while it drastically affected the results of EBMs (Fig. 5f). On the other hand, according to EBMp the thermal conduction coefficient of the nanocomposite samples follows an increasing trend with the increment of the interphase thickness (Fig. 5a), while EBMs were very sensitive to the variation of τ and did not follow any specific trend (Fig. 5d).

Moreover, the yield strength and thickness of the polymer/particle interphase region were also determined using the developed form of Zare's model based on the obtained results from the

Fig. 4 Schematic of the selective adsorptions of relatively high molar mass polymer chains onto the surface of the nanoparticles at **a** φ_d and **b** $2\varphi_d$



performed tensile tests [36]. It should be noted that development of procedure was comprised by adding the parameter μ to the computational structure of the model to involve the effects of the aggregation/agglomeration of the nanoparticles. According to the developed model, the thickness of the polymer/particle interphase region can be calculated as follows:

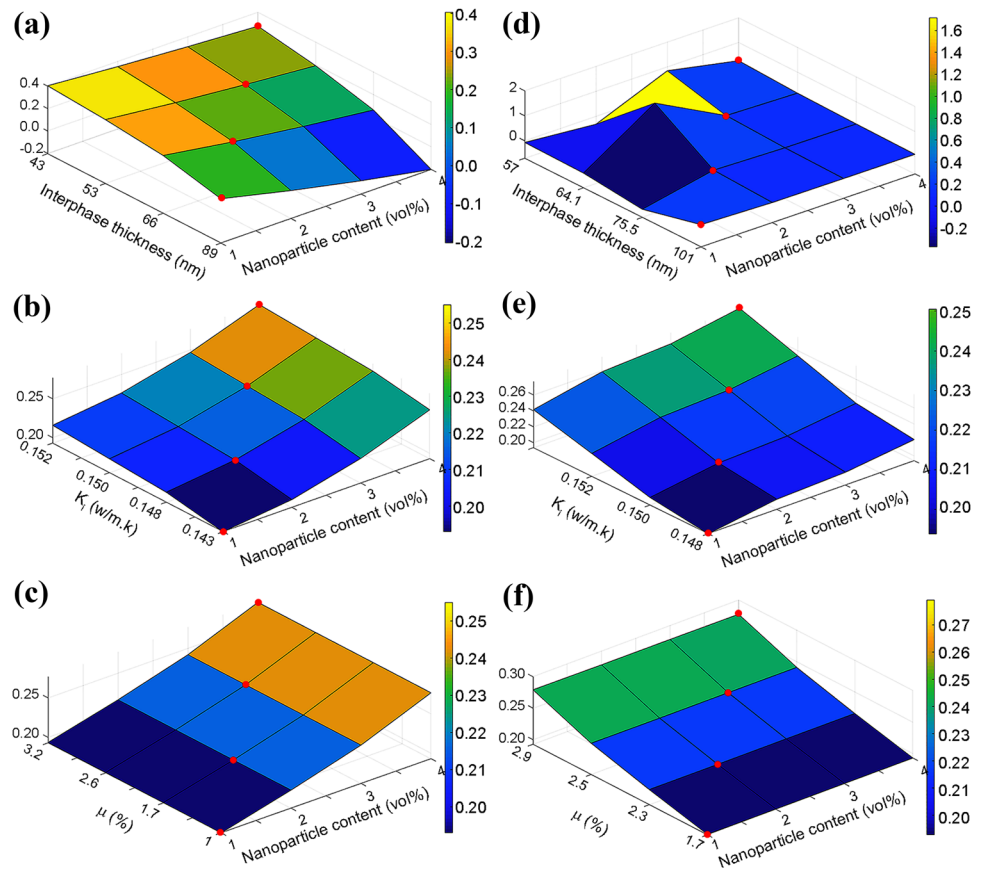
$$\tau = \frac{r}{3} \left(\frac{\ln \left(\frac{\sigma_{exp} (1 + 2.5(\mu\varphi_d)^{2/3})}{\sigma_m (1 - (\mu\varphi_d)^{2/3})} \right) (\mu\varphi_d)^{-2/3}}{\ln \left(\frac{\sigma_i}{\sigma_m} \right)} - 1 \right), \quad (22)$$

where σ_{exp} and σ_m are the experimental yield strength of nanocomposite and polymer matrix, respectively, r is the radius of the spherical nanoparticles, σ_i represents the yield strength of the polymer/particle interphase region and μ is the aggregation/agglomeration factor (Tables 1 and 2). Based on the nature of the tensile and heat conduction tests there is no need to discriminate the aggregation (strong bonding) or agglomeration (loose bonding) phenomena, since they were considered to have similar effects on the models. The increment of the nanoparticle content increased parameter μ and accordingly, at high nanoparticles content a major deviation could be seen from the ideal state, where

Table 2 Thermal characteristics of the PS-OXA and PMMA-OXH nanocomposite samples based on EBMs

	φ_d (vol%)	(τ) (nm)	(K_i) ($W\ m^{-1}\ k^{-1}$)	(μ) (%)	Experimental conduction coefficient ($K_{exp.}$) ($W\ m^{-1}\ k^{-1}$)	Theoretical conduction coefficient ($K_{the.}$) ($W\ m^{-1}\ k^{-1}$)	Error (%)
PS-OXA	0	–	–	–	0.163 ± 0.015	–	–
	1	101	0.148	1.7	0.196 ± 0.012	0.193	1.5
	2	75.5	0.152	2.3	0.224 ± 0.016	0.216	3.5
	3	64.1	0.153	2.5	0.251 ± 0.02	0.241	3.9
	4	57	0.156	2.9	0.283 ± 0.019	0.277	2.1
Average		74.4	0.152	2.35			
PMMA-OXH	0	–	–	–	0.290 ± 0.011	–	–
	1	114.7	0.252	0.9	0.425 ± 0.016	0.413	2.8
	2	88.6	0.257	1.6	0.514 ± 0.014	0.553	7.5
	3	73.9	0.263	2.1	0.607 ± 0.008	0.598	1.4
	4	65.6	0.266	2.9	0.698 ± 0.014	0.686	2.1
Average		85.7	0.259	1.875			

Fig. 5 Effects of the variation of parameters τ , K_i and μ on the thermal conduction coefficient of PS-OXA nanocomposite samples based on **a–c** EBMP and **d–f** EBMs structures



$\mu = 0$. Though, both mechanical and thermal models were designed in a way that they could minimize the final errors and offered the closest results to the actual values considering the aggregation/agglomeration factor.

We have previously proved that σ_i/σ_m was 5.9 and 4.3 for PMMA-OXH and PS-OXA nanocomposites, respectively [7, 30]. However, the variable mechanical characteristics of the interphase region, based on the aggregation/agglomeration factor of EBMs are represented in Table 3.

As can be seen in Table 3, τ decreased with the nanoparticles content, similar to the reported results in Tables 1 and 2 which also proved the effects of the nanoparticles content on the selective adsorption of the high molar mass polymer chains. It should be also noted that the

relatively higher values of τ in the case of PS-OXA samples (> 100 nm) could be attributed to the stronger interaction between APTES molecules and PS chains compared to that of HDTMS molecules and PMMA chains.

It is noteworthy to mention that, we have also reported 194 nm and 21.5 nm as the average thicknesses of the interphase region based on the tensile strength results of PS-OXA and PMMA-OXH nanocomposites, respectively [7, 30]. Comparing all of the represented results clearly showed that the thickness of the polymer/particle interphase region was completely depended on the nanoparticles content, aggregation/agglomeration factor and the type of the exerted driving force.

Table 3 Mechanical characteristics of the PS-OXA and PMMA-OXH nanocomposite samples based on parameter μ of EBMs

PS-OXA				PMMA-OXH		
φ_d (%)	σ_{exp} (Mpa)	σ_f (Mpa)	τ (nm)	σ_{exp} (Mpa)	σ_f (Mpa)	τ (nm)
0	28.6 ± 1.1	–	–	72.1 ± 1.6	–	–
1	32.9 ± 0.9	141.47	217.9	74.94 ± 1.2	442.14	78.7
2	32.3 ± 1.2	138.89	102.6	74.57 ± 1.1	439.96	33.4
3	32.2 ± 1	138.46	74.9	74.62 ± 0.9	440.25	23.9
4	31.3 ± 1.9	134.59	46.5	73.33 ± 2.3	432.64	12.1
Average (nm)			110.4	Average (nm)		37.02

Conclusion

The thermal and mechanical characteristics of the polymer/particle interphase region were interpreted from the thermal conduction and tensile tests, respectively. It was proved that the combination of EBMP and EBMs with the corresponding geometrical structure of the nanocomposites was completely capable of defining the thickness and thermal conduction coefficient of the interphase region as a function of φ_d and μ . Though, EBMs was more sensitive to the variation of μ and τ , it introduced a better choice for interpreting the thermal characteristics of the interphase region. On the other hand, the mechanical characteristics of the polymer/particle interphase region were interpreted from the tensile test results (yield strength) of the prepared PS-OXA and PMMA-OXH nanocomposites using a developed form of Zare's model. Comparing the results revealed that the interphase thickness in a nanocomposite system was dependent on the nanoparticle content, aggregation/agglomeration factor and type of the exerted driving force, and therefore, it should not be considered as a specific part of the nanocomposite system with constant characteristics (e. g. thickness, thermal conduction, tensile modulus, yield strength, etc.).

Declarations

Conflict of interest The authors declare that they have no conflicts of interest.

References

- Pesetskii SS, Bogdanovich SP (2013) Polymer composites and nanocomposites. In: Wang QJ, Chung Y-W (eds) Encyclopedia of tribology. Springer, Boston. https://doi.org/10.1007/978-0-387-92897-5_823
- Masoud EM, Liu L, Peng B (2020) Synthesis, characterization, and applications of polymer nanocomposites. *J Nanomater* 2020:5439136. <https://doi.org/10.1155/2020/5439136>
- Inamuddin M, Thomas S, Kumar Mishra R, Asiri AM (2019) Sustainable polymer composites and nanocomposites. Springer International Publishing, Switzerland
- Paublo DJ (2012) Tribology of nanocomposites. Springer-Verlag, Heidelberg
- Power AJ, Remediakis IN, Harmandaris V (2021) Interface and interphase in polymer nanocomposites with bare and core-shell gold nanoparticles. *Polymers (Basel)* 13:541
- Hodgkinson JM (2012) Testing the strength and stiffness of polymer matrix composites. In: Robinson P, Greenhalgh E, Pinho S (eds) Failure mechanisms in polymer matrix composites. Woodhead Publishing, Cambridge. <https://doi.org/10.1533/9780857095329.1.129>
- Sharifzadeh E (2019) Modeling of the mechanical properties of blend based polymer nanocomposites considering the effects of Janus nanoparticles on polymer/polymer interface. *Chinese J Polym Sci* 37:164–177. <https://doi.org/10.1007/s10118-019-2178-3>
- Sharifzadeh E, Ghasemi I, Karrabi M, Azizi H (2014) A new approach in modeling of mechanical properties of nanocomposites: effect of interface region and random orientation. *Iran Polym J* 23:835–845. <https://doi.org/10.1007/s13726-014-0276-1>
- Sharifzadeh E, Ghasemi I, Qarebagh AN (2015) Modeling of blend-based polymer nanocomposites using a knotted approximation of Young's modulus. *Iran Polym J* 24:1039–1047. <https://doi.org/10.1007/s13726-015-0391-7>
- Sharifzadeh E (2019) Modeling of the tensile strength of immiscible binary polymer blends considering the effects of polymer/polymer interface and morphological variation. *Chinese J Polym Sci* 37:1176–1182. <https://doi.org/10.1007/s10118-019-2274-4>
- Zhai S, Zhang P, Xian Y, Zeng J, Shi B (2018) Effective thermal conductivity of polymer composites: theoretical models and simulation models. *Int J Heat Mass Transfer* 117:358–374. <https://doi.org/10.1016/j.ijheatmasstransfer.2017.09.067>
- Netravali AN, Mittal KL (2016) Interface/Interphase in polymer nanocomposites. Wiley, Massachusetts
- Jesson DA, Watts JF (2012) The interface and interphase in polymer matrix composites: effect on mechanical properties and methods for identification. *Polym Rev* 52:321–354. <https://doi.org/10.1080/15583724.2012.710288>
- Ji XL, Jing JK, Jiang W, Jiang BZ (2002) Tensile modulus of polymer nanocomposites. *Polym Eng Sci* 42:983–993. <https://doi.org/10.1002/pen.11007>
- Sharifzadeh E, Amiri Y (2021) The effects of morphological variation and polymer/polymer interface on the tensile modulus of binary polymer blends: a modeling approach. *J Polym Eng* 41:109–118. <https://doi.org/10.1515/polyeng-2020-0013>
- Buryan OK, Novikov VU (2002) Modeling of the interphase of polymer-matrix composites: determination of its structure and mechanical properties. *Mech Compos Mater* 38:187–190. <https://doi.org/10.1023/A:1016008432083>
- Maghami S, Shahrooz M, Mehrabani-Zeinabad A, Zornoza B, Sadeghi M (2020) Characterization of the polymer/particle interphase in composite materials by molecular probing. *Polymer* 205:122792. <https://doi.org/10.1016/j.polymer.2020.122792>
- Jain S, Goossens JGP, Peters GWM, van Duin M, Lemstra PJ (2008) Strong decrease in viscosity of nanoparticle-filled polymer melts through selective adsorption. *Soft Matter* 4:1848–1854. <https://doi.org/10.1039/B802905A>
- Zamanian M, Ashenai Ghasemi F, Mortezaei M (2021) Interphase characterization and modeling of tensile modulus in epoxy/silica nanocomposites. *J Appl Polym Sci* 138:49755. <https://doi.org/10.1002/app.49755>
- De Gennes P-G (1976) Scaling theory of polymer adsorption. *J Phys* 37:1445–1452. <https://doi.org/10.1051/jphys:0197600370120144500>
- Zare Y, Rhee KY (2020) Study on the effects of the interphase region on the network properties in polymer carbon nanotube nanocomposites. *Polymers* 12:182
- Boyard N (2016) Heat transfer in polymer composite materials: forming processes. Wiley, New Jersey
- Thomas S, Joseph K, Malhotra SK, Goda K, Sreekala MS (2013) Polymer composites nanocomposites. Wiley, New Jersey
- Ashraf MA, Peng W, Zare Y, Rhee KY (2018) Effects of size and aggregation/agglomeration of nanoparticles on the interfacial/interphase properties and tensile strength of polymer nanocomposites. *Nanoscale Res Lett* 13:214. <https://doi.org/10.1186/s11671-018-2624-0>
- Zare Y (2016) Study of nanoparticles aggregation/agglomeration in polymer particulate nanocomposites by mechanical properties. *Compos Part A Appl Sci Manuf* 84:158–164. <https://doi.org/10.1016/j.compositesa.2016.01.020>
- Sharifzadeh E, Tohfegar E, Safajou Jahankhanemlou M (2020) The influences of the nanoparticles related parameters on the

- tensile strength of polymer nanocomposites. *Iran J Chem Eng (IJChE)* 17:65–78. <https://doi.org/10.22034/ijche.2020.234505.1337>
27. Gao S-L, Mäder E (2002) Characterisation of interphase nanoscale property variations in glass fibre reinforced polypropylene and epoxy resin composites. *Compos Part A Appl Sci Manuf* 33:559–576. [https://doi.org/10.1016/S1359-835X\(01\)00134-8](https://doi.org/10.1016/S1359-835X(01)00134-8)
 28. Ding Y, Tran KN, Gear JA, Mainwaring D, Murugaraj P (2008) The influence of interphase between nanoparticles and matrix on Young's Modulus of nanocomposites. *Procc Int Conf NanoSci NanoTechnol*. <https://doi.org/10.1109/ICONN.2008.4639237>
 29. Sharifzadeh E, Parsnasab M (2021) Direct and reverse desymmetrization process in O/W Pickering emulsions to produce hollow graphene oxide Janus micro/nano-particles. *Colloids Surf A Physicochem Eng Asp* 619:126522. <https://doi.org/10.1016/j.colsurfa.2021.126522>
 30. Sharifzadeh E, Amiri Y (2020) The effects of the arrangement of Janus nanoparticles on the tensile strength of blend-based polymer nanocomposites. *Polym Compos* 41:3585–3593. <https://doi.org/10.1002/pc.25645>
 31. Ciprari D, Jacob K, Tannenbaum R (2006) Characterization of polymer nanocomposite interphase and its impact on mechanical properties. *Macromolecules* 39:6565–6573. <https://doi.org/10.1021/ma0602270>
 32. Boutaleb S, Zaïri F, Mesbah A, Naït-Abdelaziz M, Gloaguen JM, Boukharouba T, Lefebvre JM (2009) Micromechanics-based modelling of stiffness and yield stress for silica/polymer nanocomposites. *Int J Solids Struct* 46:1716–1726. <https://doi.org/10.1016/j.ijsolstr.2008.12.011>
 33. Mittal V (2013) Modeling and prediction of polymer nanocomposite properties. Wiley, Weinheim
 34. Bergman TL, Lavine AS, Incropera FP, DeWitt DP (2011) Fundamentals of heat and mass transfer. Wiley, Jefferson
 35. Griskey RG (1995) Heat transfer in polymer systems. *Polymer process engineering*. Springer, Dordrecht
 36. Zare Y (2016) Modeling the yield strength of polymer nanocomposites based upon nanoparticle agglomeration and polymer–filler interphase. *J Colloid Interface Sci* 467:165–169. <https://doi.org/10.1016/j.jcis.2016.01.022>